IEICE TRANS. COMMUN., VOL.E104–B, NO.6 JUNE 2021

PAPER

A Study on Decoupling Method for Two PIFAs Using Parasitic Elements and Bridge Line

Quang Quan PHUNG[†a)], ***Student Member***, **Tuan Hung NGUYEN**[††], ***Nonmember***, **Naobumi MICHISHITA**[†], **Hiroshi SATO**[†††], **Yoshio KOYANAGI**[†††], ***Members***, ***and*** **Hisashi MORISHITA**[†], ***Fellow***

SUMMARY In this study, a novel decoupling method using parasitic elements (PEs) connected by a bridge line (BL) for two planar inverted-F antennas (PIFAs) is proposed. The proposed method is developed from a well-known decoupling method that uses a BL to directly connect antenna elements. When antenna elements are connected directly by a BL, strong mutual coupling can be reduced, but the resonant frequency shifts to a different frequency. Hence, to shift the resonant frequency toward the desired frequency, the original size of the antenna elements must be adjusted. This is disadvantageous if the method is applied in cases where the design conditions render it difficult to connect the antennas directly or adjust the original antenna size. Therefore, to easily reduce mutual coupling in such a case, a decoupling method that does not require both connecting antennas directly and adjusting the original antenna size is necessitated. This study demonstrates that using PEs connected by a BL reduces the mutual coupling from −6.6 to −14.1 dB, and that the resonant frequency is maintained at the desired frequency (2.0 GHz) without having to adjust the original PIFAs size. In addition, impedance matching can be adjusted to the desired frequency, resulting in an improved total antenna efficiency from 77.4% to 94.6%. This method is expected to be a simple and effective approach for reducing the mutual coupling between larger numbers of PIFA elements in the future.

key words: *PIFAs, parasitic elements, bridge line, decoupling*

1. Introduction

In recent years, multiple-input multiple-output (MIMO) has been considered as an attractive method for enhancing transmission system performance to achieve large capacity and high speed; therefore, it is a key technology in achieving next-generation communication [1]. This technique is applied not only in base stations, but also in mobile handset terminals. Therefore, the integration of multiple antennas on a mobile handset terminal has become a prerequisite, even though the space for installing multiple built-in antennas has decreased. Moreover, when antennas are closely spaced on the same ground plane, strong mutual coupling occurs between them, which adversely affects the antenna efficiency.

To date, many decoupling solutions using various arrays of conventional antenna elements have been proposed. For example, the method using slots on the ground plane to physically eliminate the current path between antenna elements is regarded as a simple method [2]–[4]; however, the space for mounting electronic components on the ground plane is reduced. In addition, placing electromagnetic band gap (EBG) structures on the ground plane is useful for suppressing electromagnetic wave propagation between antenna elements [5], [6]. However, the EBG structure requires considerable space, rendering it difficult to use it in array antennas, which are spaced closely. Other methods have been proposed [7]–[9]; however, those methods require the use of many electronic components to form the decoupling circuit. A disadvantage of the decoupling circuit is that it affects the impedance matching of antennas; therefore, to obtain impedance matching at the desired frequency, a matching circuit is required as well. Moreover, the structures of the decoupling circuit and matching circuit are complex, and the operating bandwidth is reduced significantly.

The method using a thin metal line to directly connect antenna elements is a well-known and effective decoupling method and is known by various names, such as suspended lines, neutralization lines, or bridge lines [10]–[14]. In this study, we focus on this method because its configuration is simple. For convenience, the method will be referred to as a bridge line (BL) hereinafter. Thus far, the BL has only been studied for decoupling two antenna elements. In our previous studies, connecting antennas by a BL significantly reduced the mutual coupling of two L-shaped folded monopole antennas (LFMAs) [13]. However, the resonant frequency shifts to a different frequency when the antenna elements are connected directly by a BL, particularly in the case where the antennas operate in a narrow band. Hence, to shift the resonant frequency toward the desired frequency, the original size of the antenna elements must be adjusted individually. In [14], BLs were used to connect parasitic elements instead of directly connect the feeding element of antennas; however, it requires the redesign of the original antennas. This is considered disadvantageous if the method is applied in cases where the design conditions render it difficult to connect the antenna directly or adjust the original antenna size. Therefore, to easily reduce the mutual coupling in such a case, a decoupling method that does not require both connecting antennas directly and adjusting the original antenna size is necessitated.

Herein, we propose a novel decoupling method using

Manuscript received March 31, 2020.
Manuscript revised October 12, 2020.
Manuscript publicized December 22, 2020.

[†]The authors are with the Graduate School of Science and Engineering, National Defense Academy, Yokosuka-shi, 239-8686 Japan.
[††]The author is with the Le Quy Don Technical University, Hanoi, Vietnam.
[†††]The authors are with the Panasonic Corporation, Yokohama-shi, 224-0054 Japan.
a) E-mail: em59045@nda.ac.jp

DOI: 10.1587/transcom.2020EBP3048

parasitic elements (PEs) connected by a BL. First, as a primary study, the proposed method will be investigated for two planar inverted-F antennas (PIFAs), which are generally used as built-in antennas for mobile handset terminals, to confirm the possibility of the proposed method. The simulations in this study were performed using the simulator CST, version 2020.

2. Configuration of PIFAs and Effect of BL Connected Directly to PIFAs

2.1 Configuration of PIFAs

Figure 1 shows the configuration of the two original PIFA elements mounted on a rectangular ground plane measuring 120 mm × 45 mm. The ground plane is represented as a shielding plate in a mobile handset terminal. The PIFA patches were optimized to a size of 20 mm × 19 mm such that the PIFAs resonated at a frequency of approximately 2.0 GHz (f_0). The two PIFA elements were symmetrically mounted with respect to the centerline of the ground plane and separated by 7 mm ($0.05\,\lambda_0$). They were placed 7 mm above the ground plane, and each PIFA element was fed by a 50 Ω source at the feeding pin. Moreover, to increase the space for mounting electronic components on the ground plane, which is below the PIFA patches, the feeding and shorting pins were placed at the short edge of the ground plane and arranged symmetrically to each other with respect to the centerline. An advantage of the PIFA is that its impedance matching can be easily accomplished by adjusting the positions of the feeding and shorting pins. Therefore, the distance between the feeding and short pins was set to 11 mm after performing a parametric study. The PIFA elements and ground plane were made of copper and measured 0.3 and 0.5 mm thick, respectively.

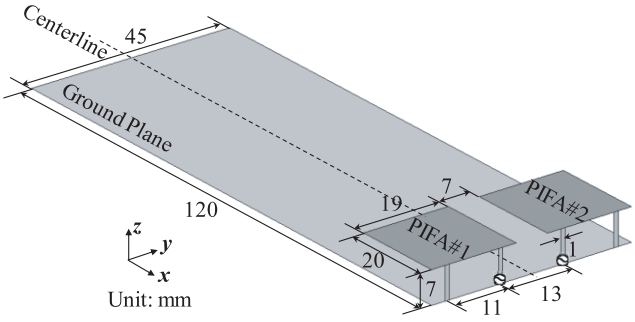

Fig. 1 Configuration of two original PIFAs.

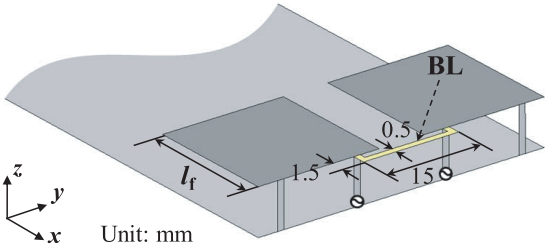

Fig. 2 Configuration of PIFAs connected directly by a BL.

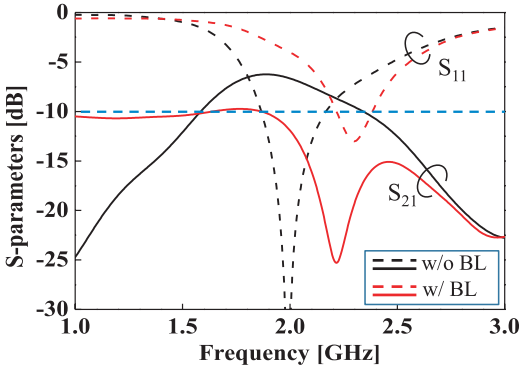

Fig. 3 S-parameters of PIFAs with and without BL.

2.2 Effect of BL Connected Directly to PIFAs

In a previous study pertaining to two LFMAs, as shown in [13], it was observed that the mutual coupling reduced but the resonant frequency shifted to a higher frequency. However, the LFMA exhibited a certain structure that might have caused a change in the resonant frequency when the antennas were connected directly by the BL. In this study, a BL was applied to two PIFAs to evaluate the effect of the BL on the resonant frequency more effectively. First, we discovered that the BL should be connected at the feeding pin of the antennas, where the currents have the highest intensity [10]. Figure 2 shows the configuration of two PIFAs connected directly to their feeding pins by the BL. The BL was positioned at the same height as the PIFAs.

Figure 3 shows the S-parameters of PIFAs with and without a BL. As shown, in the case of PIFAs without a BL, the resonant frequency was 2.0 GHz, and a strong mutual coupling (S_{21} = −6.6 dB) occurred between two PIFAs at their resonant frequencies. Meanwhile, when the PIFAs were connected by a BL, S_{21} reduced significantly at approximately 2.3 GHz. However, the resonant frequency shifted from 2.0 to 2.3 GHz, and the impedance matching deteriorated compared with the case of PIFAs without a BL. The reason contributing to the shift in the resonant frequency to a different frequency at a higher band after directly connecting the PIFAs will be explained in Sect. 4.2.

The antenna size can be increased to shift the resonance to a lower frequency. However, this may not be appropriate from the viewpoint of miniaturization but acceptable in cases where the design conditions facilitate the technique. Figure 4 shows the S-parameters when the PIFA patch length l_f is varied. As shown, the resonant frequency was 2.0 GHz when l_f = 24 mm. Furthermore, the lowest S_{21} increased when l_f increased, but it was still less than −18 dB at 2.0 GHz.

It is noteworthy that the objective of this investigation is not to determine the amount of mutual coupling that can be reduced when the PIFAs are directly connected by the

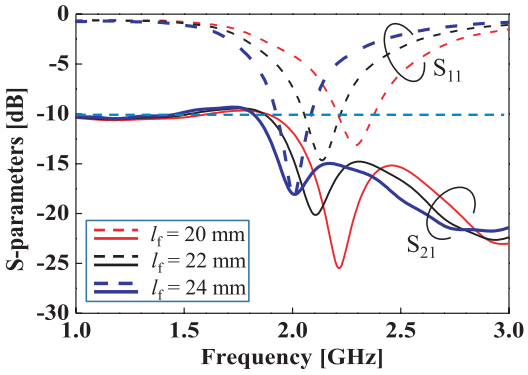

Fig. 4 S-parameters of varying PIFA patch length l_f (with a BL).

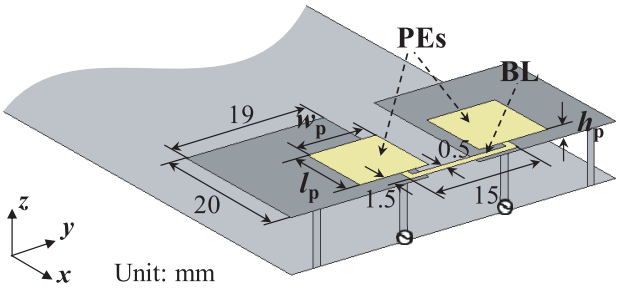

Fig. 5 Configuration of PIFAs-loaded PEs (connected by a BL).

BL. However, based on our results, we would like to emphasize the following salient points: 1) Although the LF-MAs and PIFAs had different configurations, the resonant frequencies remained similar when the abovementioned antennas were connected directly by the BL. In other words, the BL significantly affected the resonant frequency regardless of the antenna configuration; 2) when the BL was used to directly correct the antennas, the antenna size must be adjusted to shift the resonant frequency toward the desired frequency or improve the impedance matching.

As mentioned above, when the design condition enables the antennas to be directly connected by the BL and the size of the original antennas to be adjusted, then it is easy and effective to decouple the antennas using this method. However, for decoupling the antennas when the design condition is difficult to achieve, we propose another decoupling method known as parasitic elements (PEs) connected by a BL, which will be discussed in the next section.

3. Proposed Decoupling Method Using PEs Connected by BL

In this section, we present the decoupling method using PEs that are connected by a BL and loaded onto the PIFAs. Previously, PEs were generally utilized to adjust either the directivity of the antenna to the desired direction or to enhance the operating bandwidth, as discussed in [4] and [15]–[17]. Studies utilizing PEs to reduce the mutual coupling of MIMO antennas are few. Moreover, the novelty of our proposal is that the advantages of the PEs and BL are utilized to reduce the mutual coupling as well as to maintain the impedance matching at the desired frequency and the original size of the two PIFAs.

3.1 Configuration and Effects of PEs Connected by BL

Figure 5 shows the configuration of two PEs connected by a BL and then loaded onto the PIFAs. The size of each PE was $l_p \times w_p$, and the air gap between PEs and PIFAs was h_p. The spacing between the two PEs was the same as that of the two PIFAs (7 mm). The BL was used to connect them at points closest to the feeding strip of the PIFAs. To determine the optimal position and size of the PEs, we varied several parameters individually while fixing the other parameters.

First, h_p was varied to investigate the effects of the PEs on the PIFAs when the space between them was small. The reason for loading PEs onto PIFAs by a small air gap was that it does not significantly increase the volume of PIFAs with PEs. In this investigation, the dimensions of the PEs were fixed to $l_p = 10$ mm and $w_p = 9.5$ mm. As shown from the results in Fig. 6, when $h_p = 1.5$ mm, two resonances were observed; one appeared at a lower frequency, whereas the other at a higher frequency of 2.0 GHz. For convenience, we shall refer to the resonances appearing at the lower and higher frequencies as the first and the second resonances, respectively. The mutual coupling at the first resonant frequency was extremely strong. Meanwhile, the mutual coupling at the second resonant frequency was considerably reduced. Hence, we shall focus only on the second resonance for the next investigation. Moreover, the second resonance shifted to a lower frequency when h_p decreased. In particular, when h_p was 0.5 mm, a resonance with $S_{11} < -10$ dB was observed at 2.35 GHz. This resonance will shift to a frequency lower than 2.35 GHz if h_p is decreased to less than 0.5 mm; however, the shift is not significant. Therefore, h_p was fixed to 0.5 mm, and the other parameters of the PEs must be investigated to shift the resonance from 2.35 to 2.0 GHz. In this study, we investigated the size of the PEs by varying w_p and l_p. The objective of this investigation is to determine the size of PEs that enables the following two targets to be achieved simultaneously: 1) shifting the resonance from 2.35 to 2.0 GHz, and improving or at least maintaining S_{11} for less than -10 dB; and 2) maintaining S_{21} at less than -10 dB at 2.0 GHz.

Figure 7 shows the S-parameters of the PIFAs when w_p was varied from 9.5 to 25.5 mm, while l_p was fixed at 10 mm. It is obvious that, even though w_p increased considerably, the resonance only shifted slightly from 2.35 GHz to a lower frequency. Moreover, when $w_p = 25.5$ mm, S_{11} deteriorated for beyond -10 dB. Hence, it was evident that the first target of this investigation cannot be achieved by varying w_p. Therefore, w_p was fixed at 9.5 mm. Meanwhile, as shown in Fig. 8, when l_p increased from 10 to 26 mm, the resonance shifted from 2.35 GHz to a lower frequency. In particular, when $l_p = 26$ mm, the resonance appeared at 2.0 GHz, and S_{11} improved significantly for less than -30 dB. Additionally, S_{21} was maintained at less than

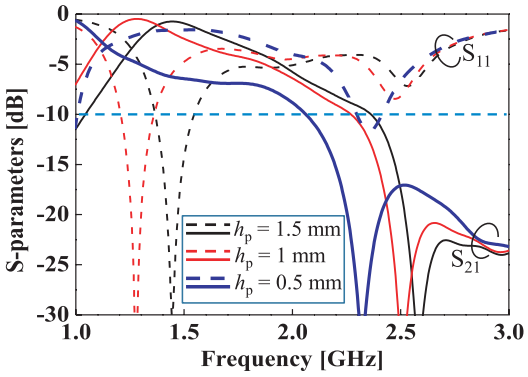

Fig. 6 Effects of varying h_p (l_p = 10 mm and w_p = 9.5 mm).

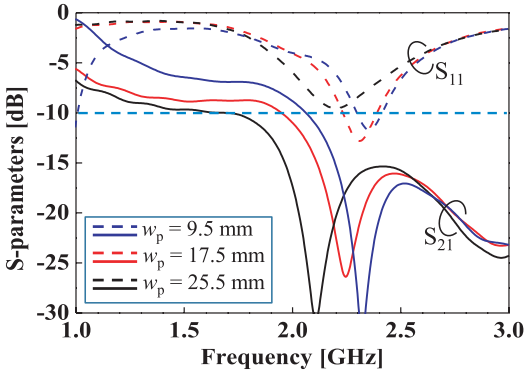

Fig. 7 Effects of varying w_p (h_p = 0.5 mm and l_p = 10 mm).

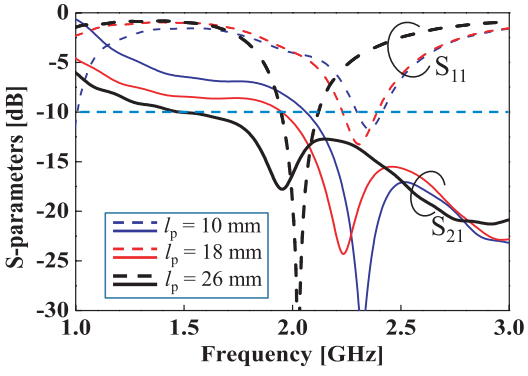

Fig. 8 Effects of varying l_p (h_p = 0.5 mm and w_p = 9.5 mm).

−16.7 dB at 2.0 GHz. Hence, the two targets of this investigation were achieved.

By varying the parameters, we can determine the optimal position and size of the PEs, where h_p = 0.5 mm, l_p = 26 mm, and w_p = 9.5 mm. The other parameters of the PEs may also affect the performances of the PIFAs, although insignificantly.

3.2 Miniaturization of PEs

By loading the PEs with the parameters determined above, a low level of mutual coupling and impedance matching was obtained at 2.0 GHz without adjusting the original size of the PIFAs. However, the volume of the PIFAs including PEs and the BL increased. Therefore, the miniaturization of PEs was considered. To achieve this, the PEs were bent at a certain position, as shown in Fig. 9(a), and the results are shown in Fig. 9(b). The total length l_p of the PEs was maintained at 26 mm in this investigation. The results demonstrate that when the PEs were bent, the resonant frequency remained unchanged. In addition, the mutual coupling level remained at 2.0 GHz for less than −10 dB. Therefore, the two targets mentioned in Sect. 3.1 were still achieved.

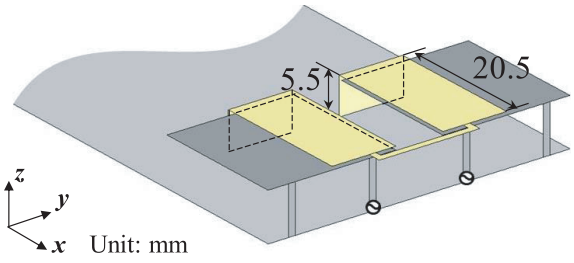

(a) Configuration of PIFA with bent PEs

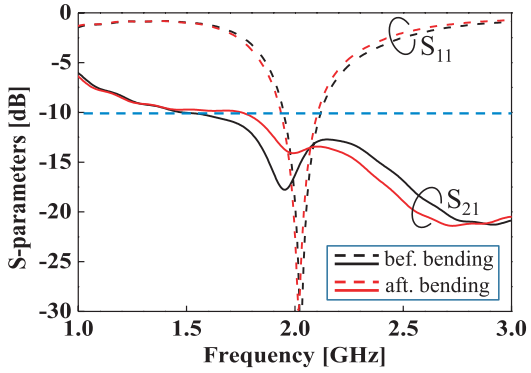

(b) S-parameters before and after bending PEs

Fig. 9 Miniaturization of PEs.

The results above show that using the PEs and BL effectively decoupled the antennas, whose feeding pins were closely spaced. It is noteworthy that if we widen the distance between ports by interchanging the position of the feeding and shorting pins of each PIFA element, then the mutual coupling will be reduced even without using PEs and the BL. However, applying the proposed method in this case can further reduce the mutual coupling.

4. Comparison of Results and Discussion

In this section, we compare the results of the PIFAs with and without PEs. By comparing the simulated and measured results, the proposed method is validated. Figure 10 shows a photograph of the fabricated PIFAs when the PEs are loaded onto them. In this prototype, two pieces of Styrofoam with a thickness of 0.5 mm were inserted between the PIFAs and PEs to maintain an air gap between them. Finally, we discuss the operating principle of the PEs by comparing the current distributions.

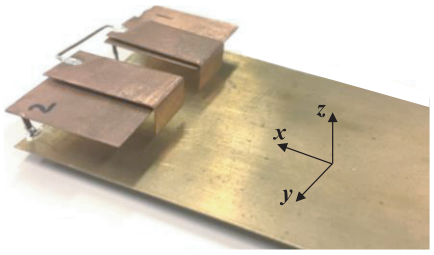

Fig. 10 Fabricated prototype of PIFAs-loaded PEs.

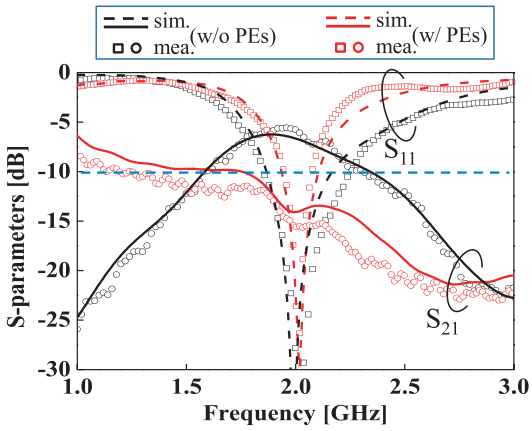

Fig. 11 Simulated and measured S-parameters of PIFAs.

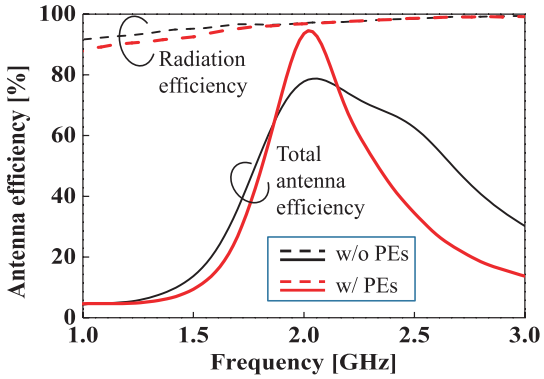

Fig. 12 Simulated radiation efficiency and total antenna efficiency of PIFAs with and without PEs.

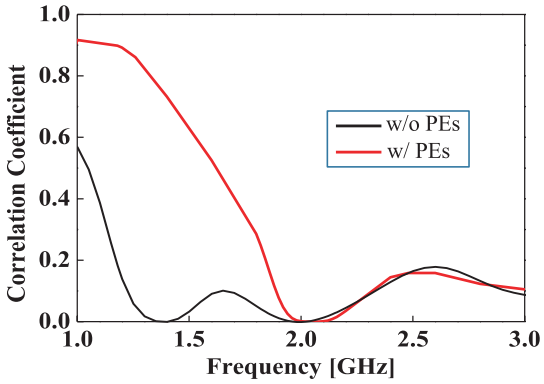

Fig. 13 Simulated correlation coefficient of PIFAs with and without PEs.

4.1 S-Parameter, Antennas Efficiencies and Correlation Coefficient

Figure 11 shows the simulated and measured S-parameters of the PIFAs with and without PEs. As shown, by loading the PEs onto the PIFAs, the mutual coupling reduced appreciably from −6.6 to −14.1 dB at 2.0 GHz. Furthermore, although the bandwidth had narrowed slightly, the resonant frequency at 2.0 GHz with good impedance matching was maintained. In addition, a good agreement was observed between the simulated and measured results; hence, the proposed method was validated.

Figure 12 shows the radiation efficiency and total antenna efficiency of the PIFAs with and without PEs, separately. The total antenna efficiency (η_{total}) is presented in Eq. (1) as follows [18]:

$$\eta_{\text{total}} = \eta_{\text{rad}}(1 - |S_{11}|^2 - |S_{21}|^2) \quad (1)$$

where η_{rad} represents the radiation efficiency, which is the ratio of the radiated power to the accepted power. Figure 12 indicated that the radiation efficiency in both cases were almost the same at the desired frequency band. Furthermore, the difference between the S_{11} in both cases at 2.0 GHz was small, as shown in Fig. 11. Thus, the total antenna efficiency mainly depends on the difference between the S_{21}. As shown, the use of PEs can improve the total antenna efficiency improved significantly from 77.4% to 94.6% at the desired frequency of 2.0 GHz by reducing the S_{21}. The correlation coefficients of the PIFAs with and without PEs are shown in Fig. 13. In the PIFAs without PEs, the correlation coefficient was initially low at 2.0 GHz. Meanwhile, using the PEs increased the correlation coefficient in the low-frequency band, but a low correlation coefficient was still maintained at the desired frequency.

4.2 Current Distributions

To understand why the resonant frequency shifts to a different frequency of higher band when the antennas are directly connected by the BL (Fig. 3) and why using PEs connected by the BL can reduce the mutual coupling, we compared the current distributions at the corresponding resonant frequency of each model. Figures 14(a), (b), (c), and (d) show the current distributions of the original PIFAs (2.0 GHz), original PIFAs connected directly by the BL (2.3 GHz), PIFAs connected directly by the BL with patch lengths l_f = 24 mm (2.0 GHz), and original PIFA-loaded PEs (2.0 GHz), respectively. In all cases, we excited port#1 and terminated port#2 by a 50 Ω load.

First, in the original PIFAs, when PIFA#1 was excited, strong currents flowed primarily on the side where PIFA#1 was located; however, a portion of those currents flowed through the ground plane and then flowed strongly into PIFA#2. This current was considered to be the main contributor to the strong mutual coupling. Herein, we re-

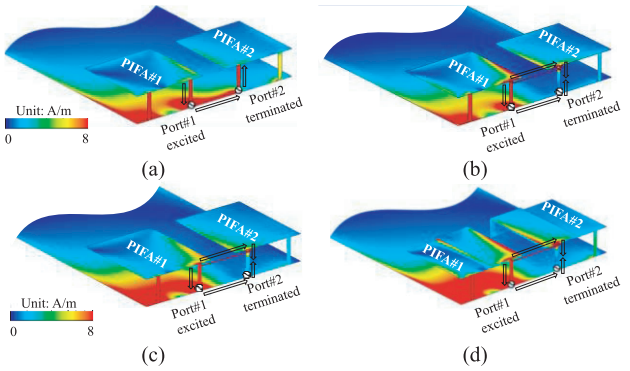

Fig. 14 Current distribution of (a) original PIFAs at 2.0 GHz, (b) original PIFAs directly connected by BL at 2.3 GHz, (c) PIFAs directly connected by BL with patches length l_f = 24 mm at 2.0 GHz, (d) original PIFAs-loaded PEs at 2.0 GHz.

fer to it as the coupling current. The coupling current adversely affected the antenna efficiency; however, it made part of PIFA#2 served as an additional radiating element when PIFA#1 was excited. In other words, when one PIFA element was excited, the currents on the ground plane and both PIFA elements enabled an operation at a resonant frequency of 2.0 GHz. However, the coupling current was canceled when the two PIFAs were connected directly by the BL, as shown in Fig. 14(b). Therefore, when PIFA#1 was excited, the current flowing on PIFA#2 and the ground plane weakened, causing the overall operating current to be reduced compared with the original PIFAs. We consider this to be the main contributor to the increase in the resonant frequency from 2.0 to 2.3 GHz. To determine how the coupling current might be canceled, we focused on the flow direction of the currents between port#1 and port#2, as shown in Fig. 14(b). It was clear that when the BL was used to directly connect the PIFAs, in addition to the current through the ground plane, other current newly appeared on the BL. The two currents canceled each other at the feeding pin of PIFA#2 because of the opposite phase. Hence, the mutual coupling between the two PIFAs reduced significantly. Furthermore, the canceled current was compensated for when the PIFA patch length l_f was increased to 24 mm, as shown in Fig. 14(c). Consequently, the resonant frequency shifted back from 2.3 to 2.0 GHz.

In the original PIFAs-loaded PEs, as shown in Fig. 14(d), a similar current distribution as that shown in Fig. 14(c) was observed. We assumed that owing to the proximity between the PEs and PIFAs, the PEs were electromagnetically affected by the PIFAs and hence behaved like radiating elements. Therefore, the role of the PEs was similar to that of the PIFAs patches. This implies that even if the PEs are connected by a BL, mutual coupling between elements can be reduced based on the principle shown in Fig. 14(c).

4.3 Radiation Patterns

The simulated and measured radiation patterns at 2.0 GHz of

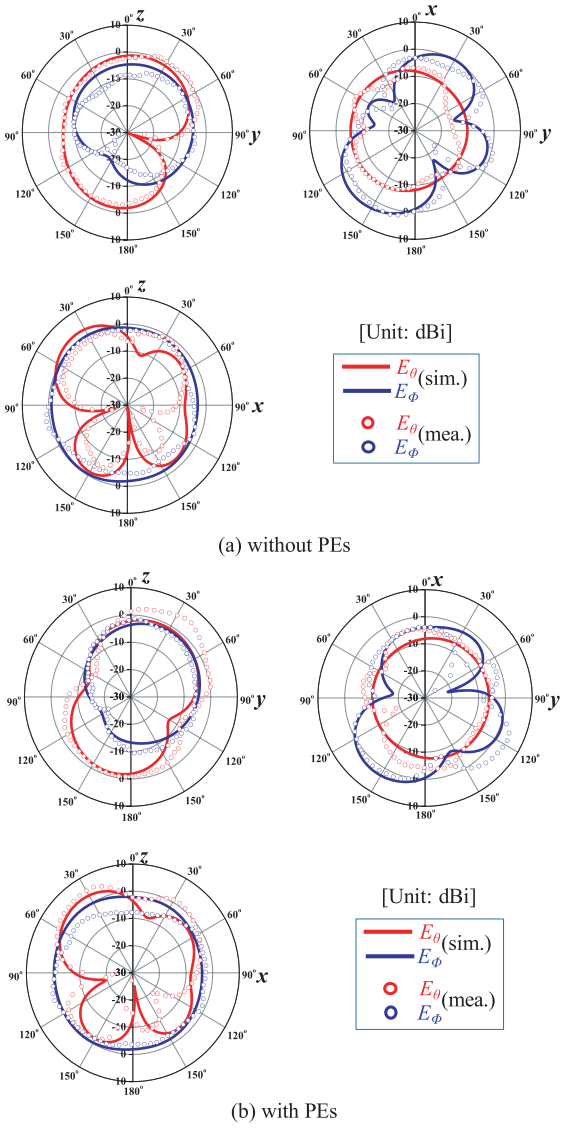

Fig. 15 Simulated and measured radiation patterns of PIFA#1 (2.0 GHz).

the PIFAs without and with PEs are shown in Figs. 15(a) and (b), respectively. Owing to the symmetrical configuration of the PIFAs, only the radiation patterns of PIFA#1 are shown. By comparing the simulated results shown in Figs. 15(a) and (b), it is clear that the radiation pattern changed at some positions, although insignificantly. In addition, the gains were still maintained in all planes when the PEs were loaded onto the PIFAs. Therefore, it can be concluded that the PEs did not significantly affect the radiation pattern of the PIFAs. Moreover, the simulated results were validated by their consistency with the measured results.

5. Confirmation of Operating Principle of PEs via CMA

Characteristic mode analysis (CMA) is known as an effective analytical method to understand the physical mechanism of antennas in detail by providing the characteristics

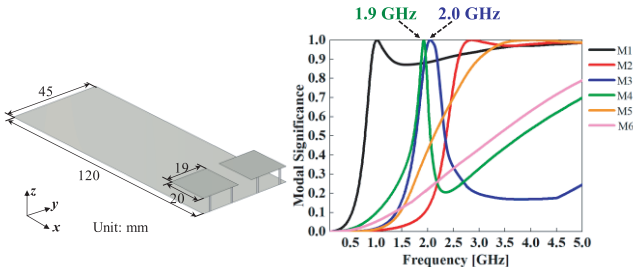

Fig. 16 Analysis model and MS of original PIFAs (before decoupling).

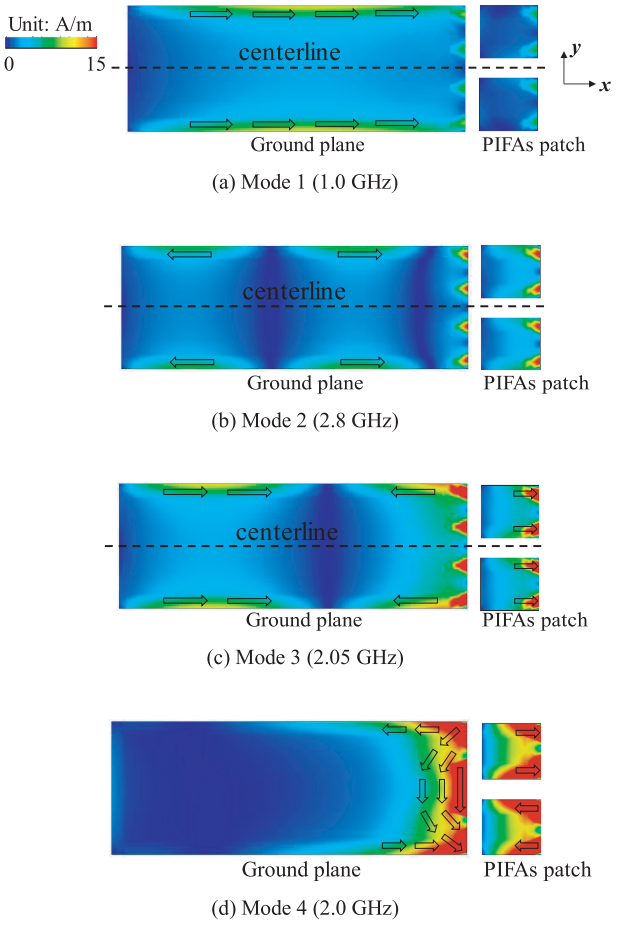

Fig. 17 Current distributions of modes before decoupling.

of modes. It has been used in several applications, including MIMO antennas [19]–[22]. In this section, CMA is presented to discuss the operation principle of the PEs in more detail. CMA is expected to facilitate the identification of the mode, which can present the mutual coupling between two PIFAs.

Figure 16 shows the analysis model and modal significance (MS) of the two original PIFAs mounted on the ground plane. In the model used in CMA, the antenna feed is excluded because the modes depend only on the antenna configuration or size. Furthermore, a mode is defined as resonant when its MS value is 1 [23]. As shown, five modes with MS = 1 appeared within the frequency range from

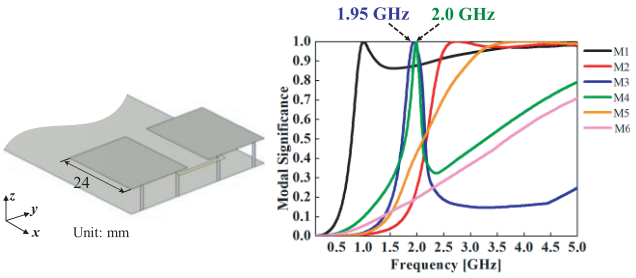

Fig. 18 Analysis model and MS of PIFAs directly connected by BL.

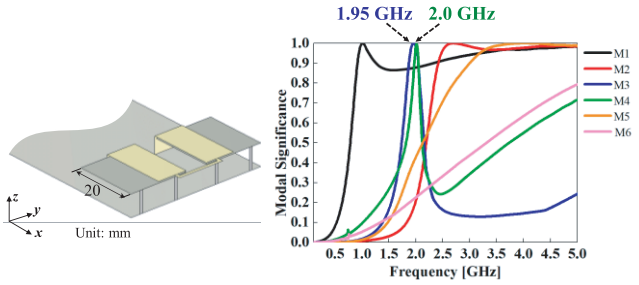

Fig. 19 Analysis model and MS of PIFAs-loaded PEs.

0.5 to 5.0 GHz. In particular, two modes (Modes 3 and 4) appeared at approximately 2.0 GHz, which is the resonant frequency of the PIFAs, as shown in the previous section. Hence, it can be concluded that the characteristics of the PIFAs are mainly dominated by modes 3 and 4. To understand the characteristics of each mode in detail, their current distributions were analyzed individually. Figures 17(a), (b), and (c) correspond to the current distributions of Modes 1, 2, and 3, respectively. It is evident that the currents flowed strongly on the long edge of the ground plane and certain positions on the PIFA patch surface. Furthermore, these currents flowed along the x-axis and were symmetric with respect to the centerline, indicating that the two PIFA elements performed similarly and were almost unaffected by each other in Modes 1, 2, and 3. Meanwhile, a distinctive characteristic is shown in Fig. 17(d), which illustrates the current distribution of Mode 4. As shown, the currents flowed strongly on the PIFA patch and the short edge of the ground plane, where the PIFAs were mounted. Moreover, the current from one PIFA element flowed through the ground plane and then flowed strongly into the other one. This current distribution was similar to that shown in Fig. 14(a). Hence, it is clear that Mode 4 resembled a special mode demonstrating mutual coupling between two PIFAs. Figures 18 and 19 show the analysis model and MS of the PIFAs directly connected by the BL and PIFAs-loaded PEs, respectively. In both cases, Mode 4 shifted from 1.9 to 2.0 GHz and appeared at almost the same frequency as Mode 3. Meanwhile, the other modes changed slightly. In other words, Mode 4 was significantly affected by the direct BL connection or the PEs loaded onto the two PIFAs. Figures 20(a) and (b) show the current distributions of Mode 4 for the two abovementioned cases. The similarity in current distribution between

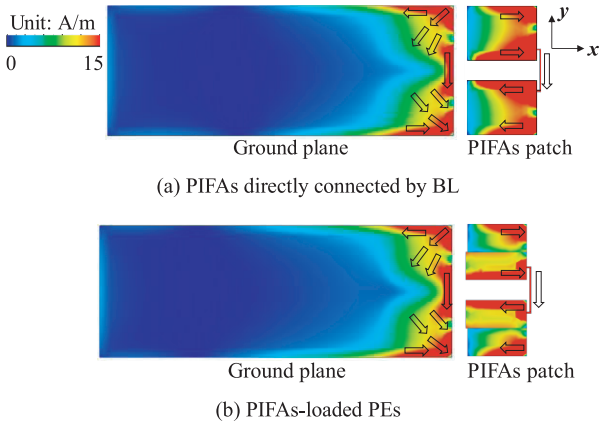

Fig. 20 Current distribution of mode 4 after decoupling (2.0 GHz).

these two cases was evident. In particular, the current flowing on the ground plane decreased compared with that of Mode 4, as shown in Fig. 17(d). Furthermore, the current flowed strongly on the BL in both cases, thereby reducing the current on the ground plane. Therefore, the operating principle of the proposed method was confirmed via CMA.

6. Conclusion

In this study, a novel decoupling method using PEs was proposed for two PIFAs in the case where the design conditions render it difficult to connect the antenna directly or adjust the original antenna size. Instead of directly connecting the antennas, a BL was used to connect the PEs, which were then loaded onto the PIFAs. Using our proposed method, the mutual coupling decreased from −6.6 to −14.1 dB, and good impedance matching was maintained simultaneously at the desired resonant frequency of 2.0 GHz without having to adjust the original sizes of the PIFAs. Therefore, the total antenna efficiency improved from 77.4% to 94.6%. Furthermore, the operating principle of the proposed method clarified that the PEs served as radiating elements, whereas the currents appearing on the BL canceled the coupling current. Additionally, the operating principle of the proposed method was discussed in detail via CMA.

In the future, we plan to improve the bandwidth and apply this decoupling method to reduce the mutual coupling of three PIFA elements.

References

[1] G.J. Foschini and M.J. Gans, "On limits of wireless communications in a fading environment when using multiple antennas," Wirel. Pers. Commun., vol.6, no.3, pp.311–335, 1998.
[2] H. Huang and J. Wu, "Decoupled dual-antenna with three slots and a connecting line for mobile terminals," IEEE Antennas Wireless Propag. Lett., vol.14, pp.1730–1733, April 2015.
[3] Y. Li, C-Y-D. Sim, Y. Luo, and G. Yang, "High-isolation 3.5 GHz eight-antenna MIMO array using balanced open-slot antenna element for 5G smartphones," IEEE Trans. Antennas Propag., vol.67, no.6, pp.3820–3830, June 2019.
[4] S. Zhang, B.K. Lau, A. Sunesson, and S. He, "Closely located dual PIFAs with T-slot induced high isolation for MIMO terminals," 2011 IEEE International Symposium on Antennas and Propagation (APSURSI), Spokane, WA, pp.2205–2207, 2011.
[5] X. Yang, Y. Liu, Y-X. Xu, and S-X. Gong, "Isolation enhancement in patch antenna array with fractal UC-EBG structure and cross slot," IEEE Antennas Wireless Propag. Lett., vol.16, pp.2175–2178, May 2017.
[6] F. Caminita, S. Costanzo, G. Di Massa, G. Guarnieri, S. Maci, G. Mauriello, and I. Venneri, "Reduction of patch antenna coupling by using a compact EBG formed by shorted strips with interlocked branch-stubs," IEEE Antennas Wireless Propag. Lett., vol.8, pp.811–814, April 2009.
[7] S.C. Chen, Y.S. Wang, and S.J. Chung, "A decoupling technique for increasing the port isolation between two strongly coupled antennas," IEEE Trans. Antennas Propag., vol.56, no.12, pp.3650–3658, Dec. 2008.
[8] S. Li and N. Honma, "Decoupling network comprising transmission lines and bridge resistance for two-element array antenna," IEICE Trans. Commun., vol.E97-B, no.7, pp.1395–1402, July 2014.
[9] T. Miyasaka, H. Sato, and M. Takahashi, "A dual-band decoupling method of 2 elements MIMO antennas by using a short stub and a branch element," IEICE Trans. Commun., vol.E102-B, no.8, pp.1763–1770, Aug. 2019.
[10] A. Diallo, C. Luxey, P. Thuc, R. Staraj, and G. Kossiavas, "Study and reduction of the mutual coupling between two mobile phone PIFAs operating in the DCS1800 and UMTS bands," IEEE Trans. Antennas Propag., vol.54, no.11, pp.3063–3073, Nov. 2006.
[11] S-W. Su, C-T. Lee, and F-S. Chang, "Printed MIMO-antenna system using neutralization-line technique for wireless USB-dongle applications," IEEE Trans. Antennas Propag., vol.60, no.2, pp.456–463, Feb. 2012.
[12] J. Itoh, N.T. Hung, and H. Morishita, "The mutual coupling reduction between two J-shaped folded monopole antennas for handset," IEICE Trans. Commun., vol.E94-B, no.5, pp.1161–1167, May 2011.
[13] Y. Kim, J. Itoh, and H. Morishita, "Decoupling method between two L-shaped folded monopole antennas for handsets using a bridge line," IET Microw. Antennas Propag., vol.4, no.7, pp.863–870, July 2010.
[14] S. Wang and Z. Du, "Decoupled dual-antenna system using crossed neutralization lines for LTE/WWAN smartphone applications," IEEE Antennas Wireless Propag. Lett., vol.14, pp.523–526, 2015.
[15] P. Jin and R.W. Ziolkowski, "High-directivity, electrically small, low-profile near-field resonant parasitic antennas," IEEE Antennas Wireless Propag. Lett., vol.11, pp.305–309, March 2012.
[16] S.T. Fan, Y.Z. Yin, B. Lee, W. Hu, and X. Yang, "Bandwidth enhancement of a printed slot antenna with a pair of parasitic patches," IEEE Antennas Wireless Propag. Lett., vol.11, pp.1230–1233, Oct. 2012.
[17] K-L. Wong, W-J. Chen, L-C. Chou, and M-R. Hsu, "Bandwidth enhancement of the small-size internal laptop computer antenna using a parasitic open slot for penta-band WWAN operation," IEEE Trans. Antennas Propag., vol.58, no.10, pp.3431–3415, July 2010.
[18] P. Hallbjorner, "The significance of radiation efficiencies when using S-parameters to calculate the received signal correlation from two antennas," IEEE Antenna Propag. Lett., vol.4, pp.97–99, June 2005.
[19] R.J. Garbacz, "Modal expansions for resonance scattering phenomena," Proc. IEEE, vol.53, no.8, pp.856–864, Aug. 1965.
[20] R.F. Harrington and J.R. Mautz, "The theory of characteristic modes for conducting bodies," IEEE Trans. Antennas Propag., vol.19, no.5, pp.622–628, Sept. 1971.
[21] D-W. Kim and S. Nam, "Systematic design of a multiport MIMO antenna with bilateral symmetry based on characteristic mode analysis," IEEE Trans. Antennas Propag., vol.66, no.3, pp.1076–1085, March 2018.
[22] K.S. Sultan, H.H. Abdullah, E.A. Abdallah, and H.S. El-Hennawy, "Metasurface-based dual polarized MIMO antenna for 5G smartphones using CMA," IEEE Access, vol.8, pp.37250–37264, Feb. 2020.

[23] M. Cabedo-Fabres, E. Antonino-Daviu, A. Valero-Nogueira, and M.F. Bataller, "The theory of characteristic modes revisited: A contribution to the design of antenna for modern applications," IEEE Trans. Antennas Propag. Mag., vol.49, no.5, pp.52–68, Oct. 2007.

Quang Quan Phung was born in Hanoi, Vietnam, on March 2, 1994. He received the B.E. degrees in the Department of Electrical and Electronic Engineering from National Defense Academy of Japan in 2018. He is currently continuing M.E. course in National Defense Academy of Japan from April, 2018. His current research interests include small antenna and decoupling technique for MIMO antennas.

Tuan Hung Nguyen was born in Nam Dinh, Vietnam, on August 2, 1985. He received the B.S., M.S. and PhD degrees in the Department of Electrical and Electronic Engineering from National Defense Academy of Japan in 2010, 2012, and 2015 respectively. He is now a lecturer in Faculty of Radio-Electronic Engineering of Le Quy Don Technical University in Vietnam. His research interests include antenna design for mobile handset devices and radars.

Naobumi Michishita received the B.E., M.E. and D.E. degrees in electrical and computer engineering from Yokohama National University, Yokohama, Japan, in 1999, 2001, and 2004, respectively. In 2004, he was a research associate at the Department of Electrical and Electronic Engineering, National Defense Academy, Kanagawa, Japan, where he is currently an associate professor. From 2006 to 2007, he was a visiting scholar at the University of California, Los Angeles. His current research interests include metamaterial antenna and electromagnetic analysis. He is a member of the Institute of Electronics, Information and Communication Engineers (IEICE), Japan. He is also members of the Japan Society for Simulation Technology and the Institute of Electrical and Electronics Engineers (IEEE). He was the recipient of the Young Engineer Award presented by the IEEE Antennas and Propagation Society Japan Chapter and the IEICE, Japan (2004 and 2005). He received the best paper award and the best tutorial paper award from the IEICE Communication Society in 2013 and 2014, respectively.

Hiroshi Sato was born in Tokyo, Japan, on August 2, 1975. He received B.S. and M.S. degree in electrical engineering from Tokyo City University, Japan, in 1998 and 2000, and Ph.D. degree in electrical engineering from Chiba University, Japan, in 2015. From 2004 to 2012, he has been with Panasonic Mobile Communication Co., Ltd., Yokosuka, Japan. And is currently a leader of the R&D project for mobile phone antennas in Panasonic Corporation, Yokohama, Japan. His research interests include small antenna, MIMO antenna and decoupling technique. He was the recipient of the Best Paper Award from the Institute of Electronics, Information and Communication Engineers (IEICE) Transactions of Japan in 2012. He is a member of IEICE and IEEE.

Yoshio Koyanagi was born in Tokyo, Japan, on August 21, 1965. He received the B.S. degree in communication engineering from The University of Electro-Communications, Tokyo, Japan in 1989 and Ph.D. degree in engineering from Chiba University, Chiba, Japan in 2003. From 1989 to 2002, he was with Matsushita Communication Industrial Co., Ltd., Yokohama, Japan, where he was engaged in design of analog and digital cellular phone antennas. From 2003 to 2013, he was with Panasonic Mobile Communications Co., Ltd., Yokohama, Japan, where he was engaged in research and development for wireless handset antennas. He is currently a leader of the R&D project for Antenna & Electromagnetic and Wireless Power Transfer solutions for kinds of wireless devices in Panasonic Corporation, Yokohama, Japan. His research interests include mobile handset antennas and MIMO antennas and EM biological effects and wireless power supply systems. Dr. Koyanagi is a member of the Institute of Electrical and Electronics Engineers, Inc. (IEEE).

Hisashi Morishita received the B.S. degree in Electrical Engineering from National Defense Academy of Japan in 1980, the M.S. and Ph.D. degrees from University of Tsukuba in 1987 and 1990, respectively. From 1990 to 1992, he worked as a research and development officer at Air Research and Development Command of Japan Air Self-Defense Force (JASDF). Since 1992, he has been with National Defense Academy and is currently a Professor in the Department of Electrical and Electronic Engineering. From 1996 to 1997, he was a Visiting Researcher at the Communications Research Laboratory, McMaster University, Canada. His research is concerned with mobile communication and small antennas. He is a fellow of IEICE and a senior member of IEEE.